

Design of an Axial Flux Permanent Synchronous Motor with Segmented Cores

Nae-Won Hwang¹, Hyun-Kyo Jung², and Dong-Kyun Woo³

¹College of Mechanical and IT Engineering, Yeungnam University, Gyeongbuk 712-749, Korea, hnw1992@ynu.ac.kr

²Department of Electrical and Computer Engineering, Seoul National University, Seoul 151-742, Korea, hkjung@snu.ac.kr

³College of Mechanical and IT Engineering, Yeungnam University, Gyeongbuk 712-749 Korea, wdkyun@yu.ac.kr

This paper presents a motor design that utilizes segmented cores in the stator. This motor employs a 20 pole 30 slot axial gap construction for in-wheel applications. Skewed magnets are employed to decrease cogging torque. Three-dimensional finite element analysis was used to analyze motor performance. In order to verify the accuracy of the design, a prototype motor was constructed, and a large range of experiments was conducted to measure the motor characteristics.

Index Terms— Axial flux permanent magnet motor, axial gap motor, motor, synchronous motor.

I. INTRODUCTION

An axial flux permanent magnet (AFPM) motor can be found in applications, in which the axial length of the machine is limited. The AFPM motor which employed a toroidal core in the stator was introduced in [1]-[6]. A stator of the AFPM motor consists only of long lamination rolled in circular form. This means that the stator slot pitch shortens toward the inner radius of the stator stack. Therefore, the manufacturing of the stator is somewhat difficult than of the stator in the radial flux permanent magnet (RFPM) motor.

An AFPM machines have both benefits and drawbacks compared with the radial flux permanent magnet machines. The space for the end windings at the inner radius is limited. The head of the end windings comes close to the rotor shaft. This can be problematic especially in small-scale AFPM and may limit the use of small pole pair numbers. The stator is more difficult to manufacture as the distance between the stator slots along the rolled lamination vary. Therefore, this paper aimed at development of an AFPM motor using a segmented core.

II. IMPROVED QUAI-3D FEM

A. Target Motor Specification

The specification of the prototype motor is shown in Table I. In the axial gap structure, there can be more than one working face from the combination of rotor and stator. In this design, the combination of one stator with one rotor was employed. The number of poles and slots was decided by taking into consideration of the space for stator winding, cogging torque. In this paper, a 20-pole 30-slot configuration was chosen.

B. Stator Design

The analysis model is shown in Fig. 1. Steel sheets are stacked. A stack is cut by wire. The concentrated winding is employed. In order to insert coil in the slot as shown in Fig. 2, the pole shoes were removed in the slot. The segmented cores from a stack of steel sheets compose the stator. The stator is laminated along the radial direction.

C. Finite Element Analysis

In order to obtain an accurate motor design, finite element analysis was used. The analysis when the motor was operated with no load and load was carried out.

III. PROTOTYPE MOTOR

In order to verify the design and demonstrate the feasibility of an AFPM motor with segmented cored, a prototype motor was manufactured based on the design. The magnets were made of NdFeB and magnetized parallel to produce a field in axial direction. The core was segmented into separate slots with trapezoidal surfaces. The stator is shown in Fig. 3

Motor experiments were carried out to verify performances which include no load and load characteristic. The no load test is performed by unloading the motor and monitoring three phase of induced voltage. The peak value of the line to line voltage is 214[V] at 400[rpm] as shown in Fig. 4. The error between the measured and simulated value is only about 2[%], which proves the accuracy of the 3D FEA calculation. In the load test, torque characteristic was measured in terms of current at different rotating speeds. Fig. 5 shows torque versus current characteristic. The calculated value is added in this figure to compare with the measured data.

Fig. 6 shows the motor efficiency map at different power and speed range. According to this plot, an efficiency above 94% was obtained during constant power region.

IV. CONCLUSION

This paper presents an AFPM motor with segmented cores. The basic design of the motor, FEA calculation, and measurement result have been introduced.

REFERENCES

- [1] C. C. Jensen, F. Profumo, and T. A. Lipo, "A low-loss permanent-magnet brushless DC motor utilizing tape wound amorphous iron," *IEEE Trans. Ind. Appl.*, vol. 28, no. 3, pp. 646–651, May/Jun. 1992.
- [2] Z. Wang, Y. Enomoto, M. Ito, R. Masaki, S. Morinaga, H. Itabashi, and S. Tanigawa, "Development of a permanent-magnet motor utilizing amorphous wound cores," *IEEE Trans. Magn.*, vol. 46, no. 2, pp. 570–573, Feb. 2010.
- [3] K. Sitapati and R. Krishnan, "Performance comparisons of radial and axial field, permanent-magnet, brushless machines," *IEEE Trans. Ind.*

- Appl., vol. 37, no. 5, pp. 1219–1226, Sep./Oct. 2001.
- [4] A. Cavagnino, M. Lazzari, F. Profumo, and A. Tenconi, “A comparison between the axial flux and the radial flux structures for PM synchronous motors,” IEEE Trans. Ind. Appl., vol. 38, no. 6, pp. 1517–1524, Nov./Dec. 2002.
- [5] G. S. Liew, N. Ertugrul, W. L. Soong, and J. Gayler, “Investigation of axial field permanent-magnet motor utilizing amorphous magnetic material,” Aust. J. Elect. Electron. Eng., vol. 3, no. 2, pp. 1–10, 2007.
- [6] W. Fei and P. C. K. Luk, “An improved model for the back EMF and cogging torque characteristics of a novel axial flux permanent-magnet synchronous machine with a segmental laminated stator,” IEEE Trans. Magn., vol. 45, no. 10, pp. 4609–4612, Oct. 2009.

TABLE I
SPECIFICATION OF AFPM MOTOR

Stator outer diameter [mm]	280
Stator inner diameter [mm]	150
Pole number	20
Number of slots	30

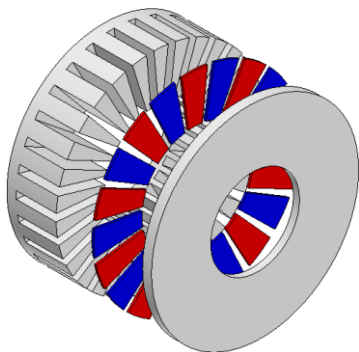


Fig. 1. The analysis model.



Fig. 2. Assembly of a coil.

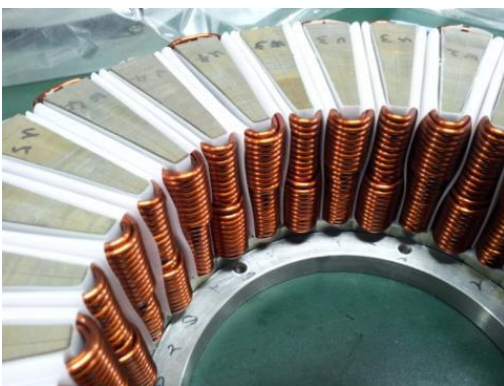
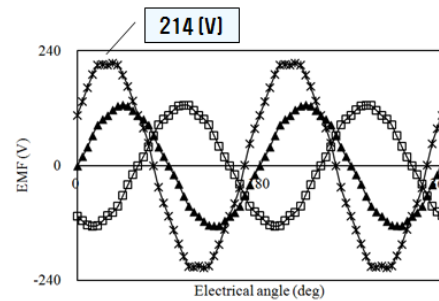
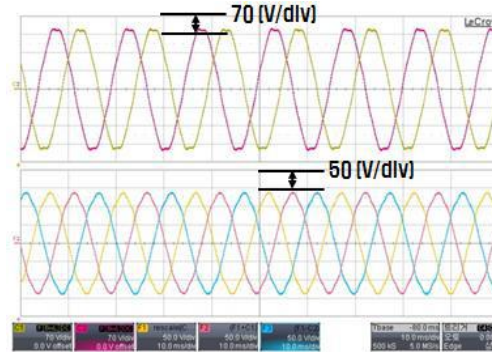


Fig. 3. The stator of prototype motor.



(a)



(b)

Fig. 4. EMF results. (a) Simulation. (b) Measurement.

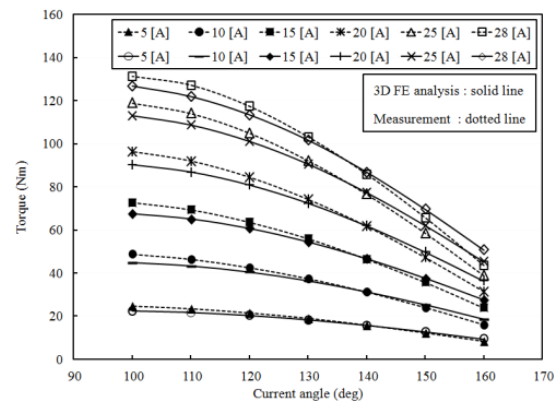


Fig. 5. Torque characteristics.

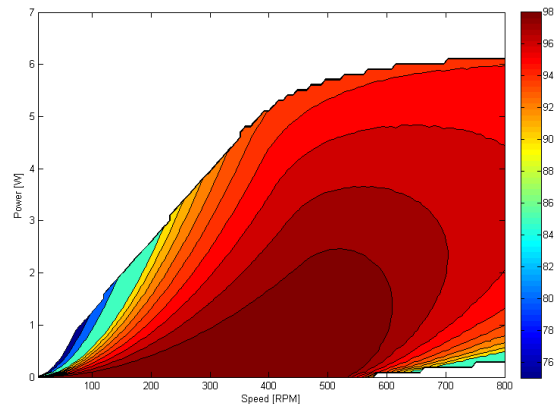


Fig. 6. Efficiency map.